Calculation of the Phase Separation Behavior of Sheared Polymer Blends

R. Horst and B. A. Wolf*

Institut für Physikalische Chemie der Universität Mainz, Jakob-Welder-Weg 13, D-W-6500 Mainz, FRG

Received March 2, 1992; Revised Manuscript Received May 28, 1992

ABSTRACT: The influence of shear on the phase diagrams of model blends of polymer A and polymer B, exhibiting phase separation upon heating, was calculated on the basis of the generalized Gibbs energy of mixing $G_{\dot\gamma}$, characterizing the steady state established at shear rate $\dot\gamma$, as the sum of G_z, the equilibrium Gibbs energy, and E_s, the energy the system can store while flowing. The results obtained for the two model systems A150/B200 and A75/B200 (the figures denote the molar masses in kg/mol) are qualitatively identical. With increasing shear rate the homogeneous region expands first, then shrinks below its equilibrium value within a certain $\dot\gamma$ range, and finally becomes again larger than with the stagnant blends. For a given composition of such a polymer mixture two regions of shear dissolution at low and at high $\dot\gamma$ values, respectively, are separated by a region of shear demixing; hence two inversion points of shear influences are theoretically expected for blends, in contrast to polymer solutions, for which one calculates only one. Experimentally, the inversion from shear dissolution to shear demixing is frequently observed and the opposite inversion was recently reported for the first time, but so far no evidence exists for the occurrence of both phenomena within the same system. Possible reasons for this fact are discussed.

Introduction

The fact that the phase separation behavior of polymer-containing liquid mixtures can markedly change as the systems flow is well-known.[1-19] Depending on the particular situation (molar mass of the macromolecules, composition of the mixture, and shear rate or elongational rate), the miscibility is either enhanced (shear dissolution) or reduced (shear demixing). A quantitative theoretical explanation[20,21] of this behavior was given for polymer solutions in terms of a generalized Gibbs energy of mixing into which the energy the system can store during its stationary flow is incorporated. With this approach it was also possible[22] to explain the experimentally observed[13] occurrence of a very special type of shear-induced two-phase region below the lower critical solution temperature (LCST), namely, the creation of a new region of immiscibility that is at some compositions separated from the original solubility gap by an interval of homogeneity; in the course of these theoretical calculations[22] it was also demonstrated that shear-induced island curves, totally segregated from the equilibrium solubility gap, can turn up in the case of LCSTs under special conditions.

All experimental observations made so far with polymer solutions could be at least rationalized, if not described quantitatively, by the mere introduction of the generalized Gibbs energy. However, recently measurements[23] with polymer blends have come to our knowledge. According to them the region of miscibility decreases with respect to the equilibrium situation upon the application of very low shear rates, whereas it increases at higher ones. Such a behavior is at variance with the results of calculations[21] performed for mixtures that also contain low molar mass components. For such systems the stored energy increases with polymer concentration more than proportionally at low shear rates (region of linear viscoelasticity), which means that this contribution to the equilibrium Gibbs energy can only undo a hump in the concentration dependence of the latter quantity; i.e., the miscibility should increase at low shear rates without exception. Furthermore, the effects should change sign as the systems flow more rapidly and the liquid becomes nonlinear viscoelastic in behavior.

The present theoretical calculation was performed to find out whether these recent experimental observations with polymer blends really contradict the approach formulated above or whether polymer mixtures exhibit some additional peculiarities, for instance, due to the fact that both components of such systems can store energy in contrast to the polymer solutions studied so far.

Theoretical Treatment of Flowing Systems

For equilibrium conditions, the binodal curve is accessible via the identity of the chemical potentials μ_i for all components i contained in the coexisting phases designated by single and double primes; for a mixture of two polymers of type A and type B, these equations read

$$\mu'_A = \mu''_A \tag{1}$$

and

$$\mu'_B = \mu''_B \tag{2}$$

Introducing a generalized Gibbs energy $G_{\dot\gamma}$ for sheared mixtures[20] according to

$$G_{\dot\gamma} = G_z + E_s \tag{3}$$

in which G_z is the zero-shear molar Gibbs energy and E_s is the energy stored in 1 mol of liquid during stationary flow, one obtains the following expressions fixing the composition of the two phases that coexist under these conditions:

$$\mu'_A + [E'_s - (\partial E_s/\partial x_B)'x'_B] = \mu''_A + [E''_s - (\partial E_s/\partial x_B)''x''_B] \tag{4}$$

and

$$\mu'_B + [E'_s + (\partial E_s/\partial x_B)'(1 - x'_B)] = \mu''_B + [E''_s + (\partial E_s/\partial x_B)''(1 - x''_B)] \tag{5}$$

Modeling of Polymer Blends

Equilibrium Phase Separation Behavior. The zero-shear chemical potentials can be calculated according to

0024-9297/92/2225-5291$03.00/0

$$\Delta\mu_A/(N_A RT) = N_A^{-1} \ln \varphi_A + (N_A^{-1} - N_B^{-1})\varphi_B + g\varphi_B^2 \quad (6)$$

and

$$\Delta\mu_B/(N_B RT) = N_B^{-1} \ln \varphi_B + (N_B^{-1} - N_A^{-1})\varphi_A + g\varphi_A^2 \quad (7)$$

N_A and N_B are the numbers of A and B segments in the two polymers, φ_i is their volume fraction in the mixture, and g is the Flory–Huggins interaction parameter, for the present calculations assumed to be independent of composition. Under this premise the expression for its critical value g_c reads

$$g_c = 0.5(N_A^{-0.5} + N_B^{-0.5})^2 \quad (8)$$

To obtain phase diagrams that can be directly compared with experimental results (i.e., in terms of the limits of miscibility as a function of temperature), assumptions have to be made concerning $g(T)$; for the subsequent calculations, performed to study mixtures near their LCST, eq 9 was used:

$$g = g_c + g_1(T - T_c) \quad (9)$$

T_c is the critical temperature and g_1 measures the exothermicity of the system.

The Stored Energy. The dependence of E_s on composition and shear rate can be formulated as[24]

$$E_s = (x_A V_A + x_B V_B)\langle J_e^\circ\rangle \langle\eta\rangle^2 \dot\gamma^2 |\langle\eta\rangle\dot\gamma|^{-2d^*} \quad (10)$$

V_A and V_B are the molar volumes of the components, $\langle J_e^\circ\rangle$ is the steady-state shear compliance, $\langle\eta\rangle$ is the viscosity of the homogeneous mixture at shear rate $\dot\gamma$, and d^* is given by

$$d^* = -(\partial \ln \langle\eta\rangle)/(\partial \ln \dot\gamma) \quad (11)$$

Knowing the zero-shear viscosity $\langle\eta_0\rangle$ and the characteristic relaxation time $\langle\tau_0\rangle$ of the blend, one can calculate both its viscosity $\langle\eta\rangle$ at a given shear rate and the parameter d^* by means of the Graessley theory[25]

$$\langle\eta\rangle/\langle\eta_0\rangle = g^{1.5}(\theta)\, h(\theta) \quad (12)$$

$$\theta = (\langle\eta\rangle/\langle\eta_0\rangle)(\dot\gamma\langle\tau_0\rangle/2) \quad (13)$$

$$g(\theta) = (2/\pi)[\operatorname{arccot}\theta + \theta/(1+\theta^2)] \quad (14)$$

$$h(\theta) = (2/\pi)[\operatorname{arccot}\theta + \theta(1-\theta^2)/(1+\theta^2)^2] \quad (15)$$

The steady-state shear compliance is given by[26]

$$\langle J_e^\circ\rangle = \langle\tau_0\rangle/\langle\eta_0\rangle \quad (16)$$

For the subsequent calculations the characteristic viscometric relaxation times of the pure components were set equal to their Rouse relaxation times[27] τ_R

$$\tau_0 = \tau_R = 6\eta_0 M/(\pi^2 \rho RT) \quad (17)$$

and the following relation was used to obtain their zero-shear viscosities:

$$\eta_0 = K[M/(\text{kg mol}^{-1})]^{3.4} \quad (18)$$

ρ is the density of the melt and K is a constant for a given temperature.

Rheological Mixing Rules. To calculate the viscosities of the homogeneous blends from those of the pure components and their weight fractions w_i in the mixture, the following relation[28] was used:

$$\langle\eta_0\rangle^{1/3.4} = w_A \eta_{0A}^{1/3.4} + w_B \eta_{0B}^{1/3.4} \quad (19)$$

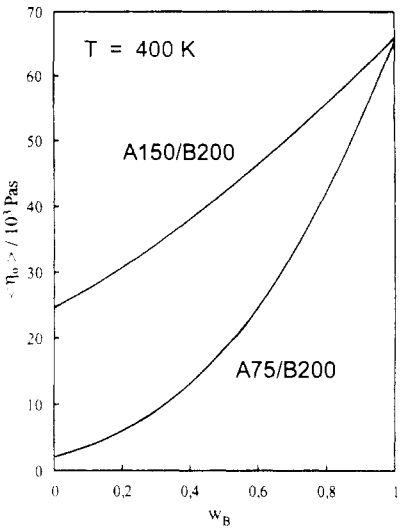

Figure 1. Zero-shear viscosity $\langle\eta_0\rangle$ of model blends of polymer A and polymer B as a function of the weight fraction w_B of component B, calculated for 400 K by means of eq 19; the figures in the designation of the systems give the masses of the polymers in kg/mol.

The analogous equation for the steady-state shear compliance of the blend reads

$$\langle J_e^\circ\rangle = (w_A \eta_{0A}^{4.4/3.4} J_{eA}^\circ + w_B \eta_{0B}^{4.4/3.4} J_{eB}^\circ)/\langle\eta_0\rangle^{4.4/3.4} \quad (20)$$

Parameters and Calculation Procedure

Two representatives of mixtures between a homopolymer A and a homopolymer B were investigated, namely, the systems A75/B200 and A150/B200; the figures after the polymers give their masses in kg/mol. The densities of both polymers were taken to be 1000 kg m^{-3}, and the volume V_s of a segment was set equal to 10^{-4} m^3 mol^{-1}. Division of the molar volumes of the polymers by V_s yields the numbers N_i of their segments. In eq 9, describing the equilibrium mixing tendency of the components as a function of temperature, a realistic value of $g_1 = 10^{-5}$ K^{-1} was chosen.

For the modeling of the rheological behavior of the systems a typical value of 10^{-3} Pa s was selected for K in eq 18 for both polymers to fix the order of magnitude of the viscosities. Furthermore, the temperature was kept constant at 400 K, i.e., close to the T_c values of the systems that are normally investigated. Figure 1 shows the concentration dependence of the zero-shear viscosity of the blend calculated by means of eqs 18 and 19 with the given parameters for the two mixtures of polymer A and polymer B of interest. The variation of the steady-state shear compliance with composition calculated from eqs 16–20 is depicted in Figure 2.

On the basis of the equations formulated in the previous sections and the numerical values of the different parameters given above, it is also possible to calculate the stored energy E_s for different shear rates and compositions of the polymer blends. To be able to apply the tools of thermodynamics to the problem as usual, one still needs an analytical expression for $E_s(x_B;\dot\gamma)$. The relation

$$E_s = E_{sA} + x_B(E_{sB} - E_{sA} - a) + a x_B^c \exp[b(1 - x_B^d)] \quad (21)$$

in which a, b, c, and d are constants that depend on shear rate was found to be very well suited for that purpose. Figure 3 demonstrates how the stored energy varies with the composition of the two blends at a given constant shear rate of 0.2 s^{-1}.

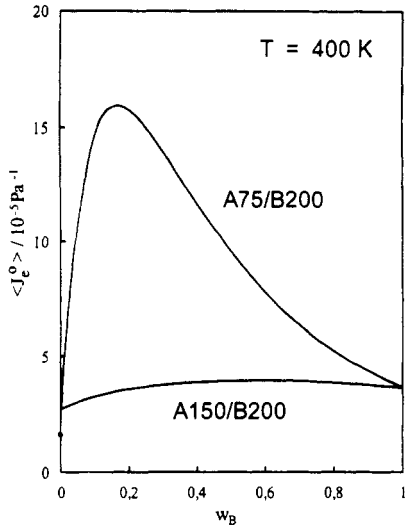

Figure 2. Steady-state shear compliance $\langle J_e^0 \rangle$ of the model blends as a function of composition calculated from eq 20 for 400 K. The point for the pure polymer A75 is given to indicate the beginning of the curve for the system A75/B200.

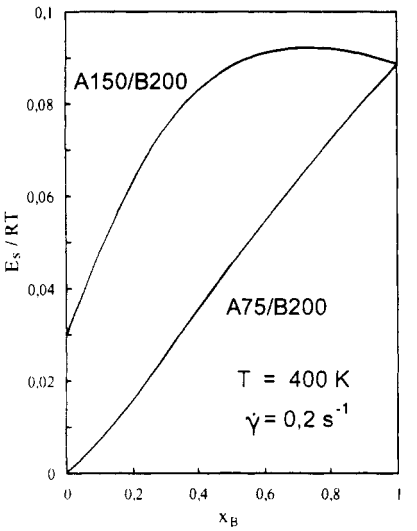

Figure 3. Reduced stored energy E_s/RT for the model blends at 400 K as a function of composition calculated for a shear rate of 0.2 s^{-1}; the drawn curves were fitted as formulated in eq 21 to the data points calculated by means of eqs 10–20.

By means of the analytical expression resulting upon the insertion of the different equations given above for the generalized Gibbs energy of mixing (isothermal conditions and constant shear rate) as a function of composition, phase diagrams of the sheared polymer blends were calculated on an IBM AT personal computer with a program written in TURBO-Pascal.[22] The algorithm is the following: For fixed values of the different system-specific parameters, x'_B and x''_B of eqs 4 and 5 are iterated until the double tangent to $G\dot{\gamma}(x_B;T,\dot{\gamma})$ is found. For well-chosen starting conditions, the required time normally amounts to a few seconds only.

Results

A150/B200. The phase diagrams obtained from these calculations for the polymer blend for which the molar masses of the components differ only moderately are shown in Figure 4. This graph shows two scales for the ordinate. On the left side the information is given in general terms; i.e., from it one can read where the phase boundaries lie in the quiescent state or at the indicated shear rates under certain equilibrium thermodynamic conditions fixed by

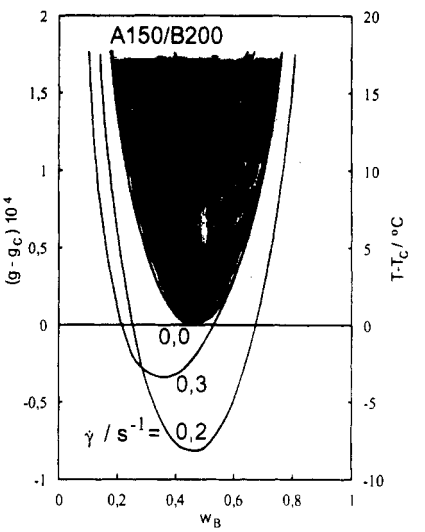

Figure 4. Phase diagrams calculated for a model blend of polymer A and polymer B (masses 150 and 200 kg/mol, respectively) at zero shear (shaded area) and at the indicated shear rates; g is the Flory–Huggins parameter (fixed by a chosen temperature T) and g_c is the critical value of the system (at the critical temperature T_c). The $T - T_c$ values on the right-hand side of the ordinate result for $g_1 = 10^{-6}$ K^{-1} in eq 8. w_B is the weight fraction of polymer B.

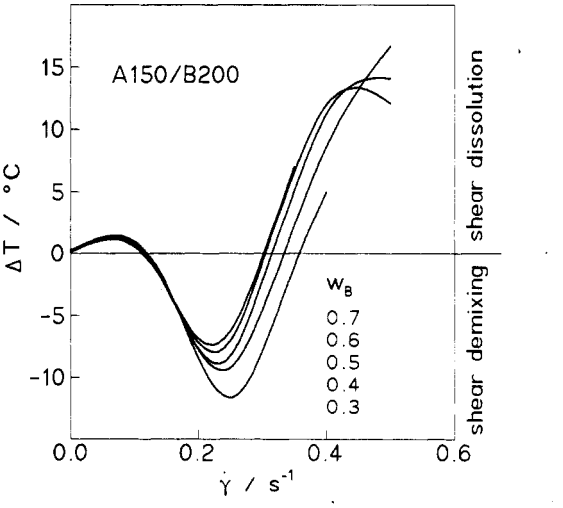

Figure 5. ΔT, deviation of the phase separation temperature of a sheared blend from its equilibrium value, as a function of shear rate $\dot{\gamma}$ calculated for the model blend A150/B200 at the different indicated weight fractions of component B.

the actual temperature (p = constant) and measured by the distance of the interaction parameter g from its critical value. On the right-hand side the results are translated by means of the g_1 value of eq 9 into an actual temperature axis, again normalized to the critical condition.

The equilibrium solubility gap of the system is given prominence by shading it. Since the components are similar in chain length, the critical composition is situated approximately in the center of the phase diagram. As one can read from the alteration in the position of the solubility gap resulting with the indicated shear rates, the two-phase region first contracts slightly as $\dot{\gamma}$ is raised, reexpands thereafter, and finally shrinks again. The situation can be more clearly seen from Figure 5, in which the change in the phase separation temperature is plotted as a function of shear rate for different constant compositions of the blend. With each dependence two inversions are observed; i.e., the effects change sign at two characteristic shear rates.

How sensitive the present blend is against shear-induced changes of the phase separation behavior at different

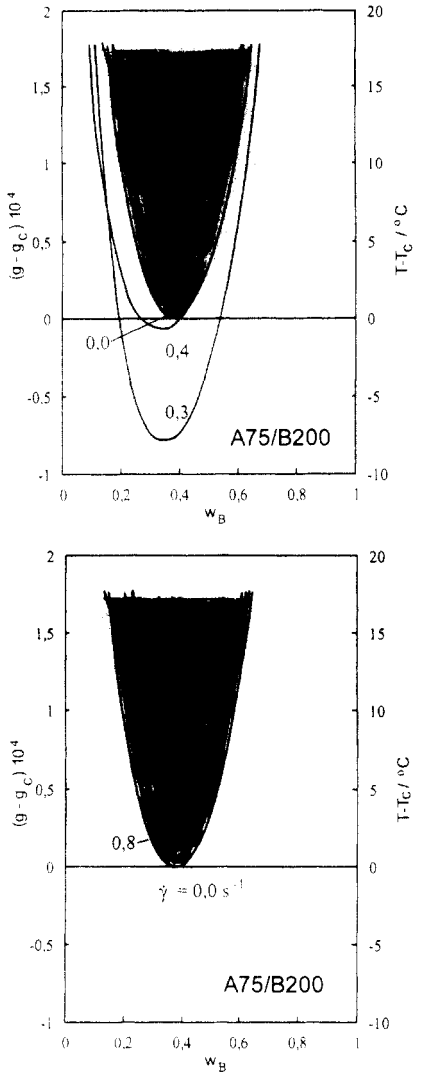

Figure 6. Phase diagrams calculated for a model blend of polymer A and polymer B (masses 75 and 200 kg/mol, respectively) at zero shear (shaded area) and at the indicated shear rates $\dot{\gamma}$.

compositions can be seen from Figures 4 and 5. The calculations demonstrate that effects turn up in a wide mixing range; they are comparable in magnitude at low shear rates, whereas with mixtures rich in A, shear demixing is particularly pronounced at intermediate shear rates while with mixtures rich in B, shear dissolution is prominent at high $\dot{\gamma}$ values.

A75/B200. For this model blend the molar masses of the components were chosen distinctly different (A, 75 kg mol^{-1}; B, 200 kg mol^{-1}) to study the transition from polymer blends to polymer solutions. The phase diagrams calculated for this mixture are shown in Figure 6. Since the influence of shear is even more complex with the present system than with the previous one, the results for low and for high $\dot{\gamma}$ values are given in separate drawings.

As $\dot{\gamma}$ increases, the following phenomena are again successively observed: shear dissolution, shear demixing, and shear dissolution. Moreover, with this blend it is clearly discernible that the effects start to level off at the highest shear rates. This situation can be more directly seen from Figure 7, which also reveals a marked influence of composition on the maximum extent of shear demixing. The effects of shear are with this blend—irrespective of its sign—most pronounced for mixtures in which the higher molecular weight component is the solute and the lower the solvent.

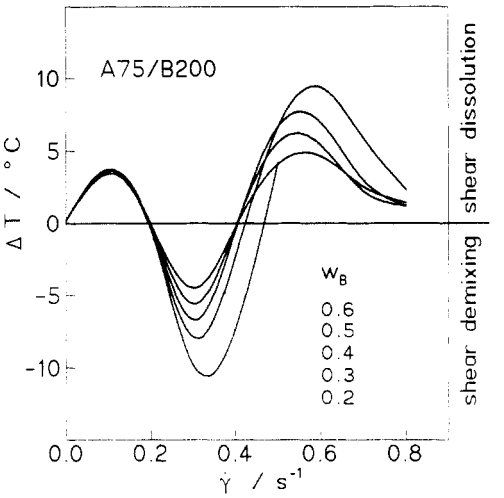

Figure 7. ΔT, deviation of the phase separation temperature of a sheared blend from its equilibrium value, as a function of shear rate $\dot{\gamma}$ calculated for the model blend A75/B200 at the different indicated weight fractions of component B.

Discussion

Comparison of the Calculations for Blends and for Solutions. The most obvious difference between these two types of systems lies in the magnitude of the effects and the concentration range over which they extend. These observations can be rationalized by the fact that E_s is larger for blends than for solutions and that $G_z(x)$ and $E_s(x)$ are much less curved in the former case than in the latter. The much broader maxima of $E_s(x)$ of polymer mixtures are most likely also the reason why eulytic points[21] did not show up for the present model blends. The curvature in this function is too small to create a second hump in $G\dot{\gamma}(x)$ that is necessary for the coexistence of three phases in flowing systems.

A further remarkable outcome of the present calculations is the second inversion of effects at high $\dot{\gamma}$ values, which is absent for polymer solutions. The explanation of this feature lies in the fact that the composition at which the maximum energy can be stored during stationary flow moves from mixtures rich in B to mixtures rich in A as the shear rate increases without becoming vanishingly small. The fact that the lower molecular weight species can also store noteworthy amounts of energy means that this maximum remains effective even when situated on the "solvent side" of the critical point. Consequently, two $\dot{\gamma}$ regions of shear dissolution—separated by a region of shear demixing—will occur with blends. With polymer solutions the second regime of shear dissolution cannot be observed, since the solutions are unable to store sufficient energy as soon as the number of entanglements per molecule becomes vanishingly small; furthermore, the maximum of E_s cannot be positioned such that, as $\dot{\gamma}$ is raised, it is situated at considerable lower than critical polymer concentrations.

In contrast to recent calculations for polymer–solvent systems exhibiting lower critical solution temperatures, no island curves were found for the present polymer blends. This, however, is only due to the details of the theoretical assumptions. Regions of shear-induced immiscibility that are separated from the equilibrium solubility gap by a region of homogeneity[22] can only be expected if E_s is treated temperature dependent such that it becomes larger as the solvent quality improves. Because of the relaxation times that increase upon a reduction of T, the occurrence of island curves is expected for favorable conditions.

Comparison of the Calculations for Blends with Experiments. The result of the theoretical considerations

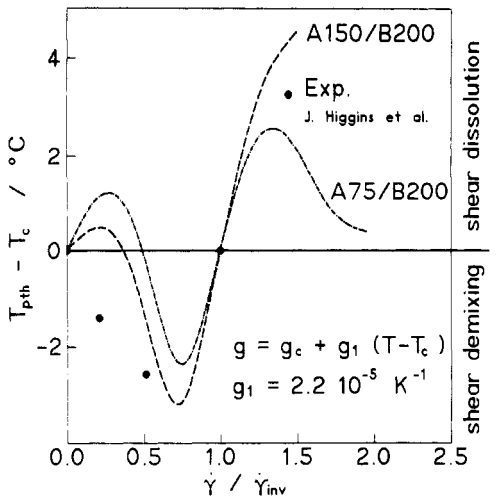

Figure 8. Differences between T_{pth}, the precipitation threshold temperature, and T_c, the critical temperature (zero shear), as a function of the shear rate $\dot{\gamma}$ reduced to $\dot{\gamma}_{inv}$, the shear rate of the inversion from shear demixing to shear dissolution, for the two model blends and for experimental data taken from the literature. For this comparison the theoretical curves were calculated with the T dependence of the Flory–Huggins interaction parameter formulated in the graph.

that upon the application of successively higher shear rates a region of shear dissolution should be followed by a region of shear demixing is in good agreement with numerous experimental findings. To our knowledge, the predicted second inversion, the reoccurrence of shear dissolution at the highest shear rates, has so far not been found with systems also showing the first inversion. However, as stated in the Introduction, it was recently reported[23] that for mixtures of a homopolymer and a copolymer one only observes the latter inversion.

The fact that the behavior calculated for the highest shear rates has not yet been observed experimentally could simply lie in the limited $\dot{\gamma}$ ranges studied so far. On the other hand, the discrepancies at low shear shear rates deserve a more detailed discussion. For this purpose a reduced description of calculated and measured effects is given in Figure 8. In this graph the abscissa is normalized to the shear rate $\dot{\gamma}_{inv}$ at which the systems change from shear demixing to shear dissolution. For the sake of simplicity the diagram does not show the changes in the phase separation temperatures for a given blend of constant composition, but rather the difference between the precipitation threshold temperature T_{pth} and the critical temperature T_c.

The agreement between experiment and theory that can be achieved by the assumption of a reasonable value for g_1 in eq 9 is not too bad if one ignores the fundamentally different behavior at low shear rates. Several explanations can be offered for that discrepancy. First, one has to look for theoretical deficiencies. One suspect could be that the energy stored in the system while it flows as compared with the Gibbs energy of mixing is so large for blends that the equations cannot be applied in the present form. However, even if this aspect could become of importance at the highest shear rates where E_s can amount to several percent of G_z, it can be ruled out for the low shear rates discussed here. Two other theoretical explanations appear more likely.

(i) Neither the effects of molecular and chemical nonuniformities of the polymers nor special situations to be expected for homopolymer/copolymer systems were incorporated. One example for the latter aspect could, for instance, be the destruction of thermodynamically favored contacts between certain monomeric units prevailing in the stagnant systems as the systems flow. Under this assumption it would be possible to construct situations in $E_s(x;\dot{\gamma})$ that eliminate the initial shear dissolution but leave the behavior at high shear rates more or less unchanged.

(ii) Another aspect concerns rheological effects associated with critical fluctuations which show up in a particularly broad range of composition with blends. Due to this additional increase in viscosity and due to the critical slowing down of molecular mobility one can postulate a further contribution to E_s, not taken into account so far, which is largest at the critical composition and consequently acts toward shear demixing. However, on the basis of experimental evidence, this explanation cannot be general, and one would still have to postulate that this contribution is particularly large with special systems.

Finally, a trivial dissolution of this qualitative discrepancy between theory and experiment can presently also not be ruled out. It could still be that even homopolymer/copolymer mixtures start with shear dissolution at the lowest shear rate and that this behavior has not yet been observed only because no experiments have been performed in this region.

Conclusions

A common assessment of the present theoretical calculations for polymer blends and the previous one dealing with polymer solutions shows the following.

Low shear rates yield in all cases shear dissolution, as long as one does not introduce special mechanisms modifying the normal storage of energy during stationary flow via entanglements. Depending on the particular thermodynamical and rheological characteristics of the system, it is possible that three phases coexist (at the eulytic points) and that island curves show up (with exothermal heats of mixing) in this $\dot{\gamma}$ range.

Increasing the shear rate changes the sign of the effects in all cases. The reason is that disentanglement processes, i.e., nonlinear viscoelastic effects, set in. For solutions these phenomena are limited to the polymer, and in the case of blends they start predominantly for the component with the larger viscometric relaxation time. This situation leads to maxima in $E_s(x;\dot{\gamma})$ that move toward the more mobile component as $\dot{\gamma}$ is raised. As soon as these maxima hit the sensitive region around the critical composition of the system, shear demixing sets in.

For polymer solutions, no further effects can be produced by an additional increase of $\dot{\gamma}$ since it is impossible to create a maximum in E_s on the solvent side of critical composition that would be required to eliminate the curvature in $G_z(x)$ producing phase separation; due to the high dilution the molecules are already disentangled and unable to store reasonable amounts of energy. The situation is, however, totally different for blends, where the molecular mass of both components exceeds the entanglement value. Under this condition the effect of shear dissolution observed at low shear rates because of the maximum in E_s, situated close to the component with the higher τ_0 value, is again setting in as soon as this maximum has passed the critical region and is now situated on the other side of the phase diagram.

In this paper and in preceding contributions it was demonstrated that the simple approach of introducing a generalized Gibbs energy by adding the energy stored in the system while it flows can predict a multitude of phenomena. The most prominent are (i) a sequence of inversions of the effects of shear that is characteristic for the type of system, (ii) island curves near LCSTs, and (iii)

the coexistence of three liquid phases under specific conditions. Further experimental studies are required to check the necessity of modifications in the theoretical treatment; such work is presently being carried out in our laboratory for ternary systems.

Acknowledgment. We are grateful to the Deutsche Forschungsgemeinschaft for support of this work. We also thank Prof. J. S. Higgins for making her typescript (ref 23) available to us prior to publication.

References and Notes

(1) Silberberg, A.; Kuhn, W. *Nature (London)* **1952**, *170*, 450.
(2) Breitenbach, J. W.; Wolf, B. A. *Makromol. Chem.* **1968**, *117*, 163.
(3) ver Strate, G.; Philipoff, W. *J. Polym. Sci., Polym. Lett. Ed.* **1974**, *12*, 267.
(4) Schmidt, J. R.; Wolf, B. A. *Colloid Polym. Sci.* **1979**, *257*, 1188.
(5) Krämer, H.; Wolf, B. A. *J. Polym. Sci., Polym. Lett. Ed.* **1980**, *18*, 789.
(6) Rangel-Nafaile, C.; Metzner, A. B.; Wissbrun, K. F. *Macromolecules* **1984**, *17*, 1187.
(7) Onuki, A. *Phys. Rev. A* **1986**, *34*, 3528.
(8) Lyngaae-Jorgensen, J.; Sondergaard, K. *Polym. Eng. Sci.* **1987**, *27*, 351.
(9) Edler, G.; Janeschitz-Kriegel, *H. Colloid Polym. Sci.* **1988**, *266*, 1087.
(10) Rector, L. P.; Mazich, K. A.; Carr, S. H. *J. Macromol. Sci., Phys.* **1988**, *B27*, 421.
(11) Bhattacharjee, S. M.; Fredrickson, G. H.; Helfand, E. *J. Chem. Phys.* **1989**, *90*, 3305.
(12) Takebe, T.; Sawaoka, R.; Hashimoto, T. *J. Chem. Phys.* **1989**, *91*, 4369.
(13) Katsaros, J. D.; Malone, M. F.; Winter, H. H. *Polym. Eng. Sci.* **1989**, *29*, 1434.
(14) Vshivkov, S. A.; Pastukhova, L. A.; Titov, R. V. *Polym. Sci. USSR (Engl. Transl.)* **1989**, *31*, 1541.
(15) Hess, S.; Loose, W. *Ber. Bunsen-Ges. Phys. Chem.* **1990**, *94*, 216.
(16) Nakatani, A. I.; Kim, H.; Han, C. C. *J. Res. Natl. Bur. Stand.* **1990**, *95*, 7.
(17) Barham, P. J.; Keller, A. *Macromolecules* **1990**, *23*, 303.
(18) Yanase, H.; Moldenaers, P.; Mewis, J.; Abetz, V.; van Egmond, J.; Fuller, G. G. *Rheol. Acta* **1991**, *30*, 89.
(19) Criado-Sancho, M.; Jou, D.; Casas-Vázquez, J. *Macromolecules* **1991**, *24*, 2834.
(20) Wolf, B. A. *Macromolecules* **1984**, *17*, 615.
(21) Krämer-Lucas, H.; Schenck, H.; Wolf, B. A. *Makromol. Chem.* **1988**, *189*, 1613, 1627.
(22) Horst, R.; Wolf, B. A. *Macromolecules* **1991**, *24*, 2236.
(23) Hindawi, I. A.; Higgins, J. S.; Weiss, R. A., private communication.
(24) Wolf, B. A. *Makromol. Chem., Rapid Commun.* **1987**, *8*, 461.
(25) Graessley, W. W. *Adv. Polym. Sci.* **1974**, *16*, 1.
(26) Laun, H. M. *Prog. Colloid Polym. Sci.* **1987**, *75*, 11.
(27) Rouse, P. E. *J. Chem. Phys.* **1953**, *21*, 1272.
(28) Schuch, H. *Rheol. Acta* **1988**, *27*, 384.